

INSTABILITY PHENOMENA IN MICROCRYSTALLINE SILICON FILMS

F. Finger^{*}, R. Carius, T. Dylla, S. Klein, S. Okur^a, M. Günes^a

Institute of Photovoltaics, Forschungszentrum Jülich, 52425 Jülich, Germany

^aIzmir Institute of Technology, Department of Physics, Urla, 35437 Izmir, Turkey

Microcrystalline silicon ($\mu\text{c-Si:H}$) for solar cell applications is investigated with respect to the material stability upon treatment of the material in various environments, followed by annealing. The material can be separated into two groups: (i) material with high crystalline volume fractions and pronounced porosity which is susceptible to in-diffusion of atmospheric gases, which, through adsorption or oxidation affect the electronic properties and (ii) compact material with high or low crystalline volume fractions which show considerably less or no influence of treatment in atmospheric gases. We report the investigation of such effects on the stability of $\mu\text{c-Si:H}$ films prepared by plasma enhanced chemical vapour deposition and hot wire chemical vapour deposition.

(Received December 9, 2004; accepted January 26, 2005)

Keywords: Microcrystalline silicon, Instability, Electron Spin Resonance

1. Introduction

Solar cells containing $\mu\text{c-Si:H}$ as an absorber layer show their highest efficiency if the material is grown near the threshold between microcrystalline and all-amorphous structure growth [1 - 3]. This could be related to the defect density and porosity of $\mu\text{c-Si:H}$ in materials with a high crystalline volume fraction. It was already reported in a very careful and detailed investigation on $\mu\text{c-Si:H}$, by Vepřek and co-workers [4], that atmospheric gas adsorption and/or oxidation affect the surface states, electronic transport, and electron spin density. A number of reports about such phenomena in $\mu\text{c-Si:H}$ have been presented in the meantime (see e.g. [5-10] and references therein). It will be important to investigate and identify these effects in state-of-the-art $\mu\text{c-Si:H}$ material prepared by PECVD and HWCVD. In particular, as is generally observed, that deposition conditions which lead to the technologically-needed higher deposition rates tend to enhance a porous structure [9]. Also, attempts to grow material with a large grain size, usually at higher deposition temperatures, in order to improve the carrier mobility, frequently result in porous material with poor grain boundary passivation.

We distinguish between type I and type II material, which are in many but not all aspects equivalent with porous (type I) and compact (type II) material. Compare the schematic presentation in Fig. 1. In type I material which has usually high crystalline volume fractions and large grain sizes, we observe crystalline columns separated by deep cracks (visible in TEM cross section images), strong Si-O absorption modes at around 1100 cm^{-1} in the infrared spectra, and a predominant Si-H stretching mode at 2100 cm^{-1} indicative of H bonded on surfaces and high spin densities (N_S), at or above 10^{17} cm^{-3} . Such material, if implemented into solar cells, yields poor efficiencies. Type II material, which is prepared under conditions closer to all-amorphous growth and which has smaller grain sizes and sometimes distinguishable amorphous volume fractions, also shows a columnar structure with deep cracks in cross section TEM. However, it does not show (or very little) Si-O absorption bands, has predominant 2000 cm^{-1} Si-H stretching modes indicative of hydrogen in a

*Corresponding author: f.finger@fz-juelich.de

compact environment, has spin densities as low as 10^{16}cm^{-3} and yields higher solar cell efficiencies. It is clear that such simple categories will not be sufficient to resolve all instability effects. Some phenomena occur in both types, but others may need a further detailed distinction, maybe even not based on material structure features.

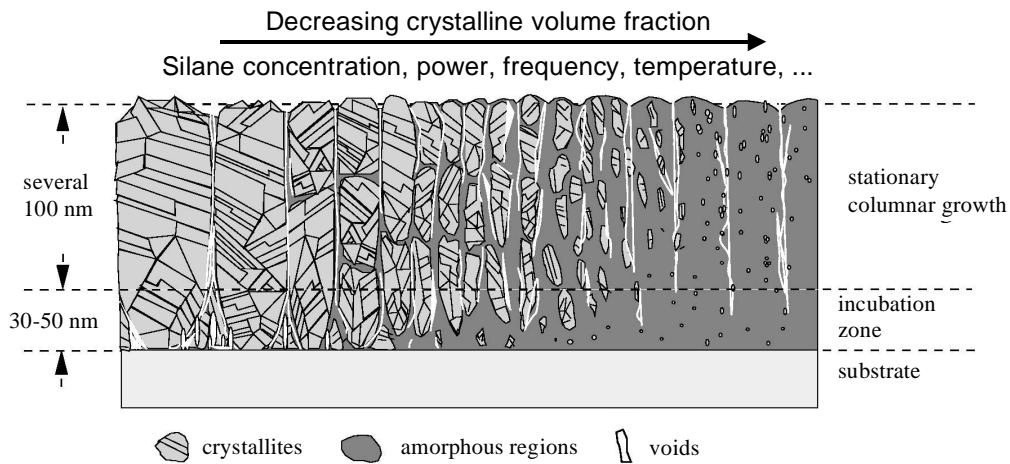


Fig. 1. Schematic diagram showing the prominent microstructure features of $\mu\text{c-Si:H}$. From left to right, the film composition changes from highly crystalline to predominantly amorphous (from ref [1]).

2. Experimental details

The PECVD material was prepared at 95 MHz. For HWCVD, we used tantalum wires. Silane-hydrogen mixtures were used as process gases. The silane concentration $SC = [\text{SiH}_4] / ([\text{SiH}_4] + [\text{H}_2])$ was varied to obtain material in the entire range from highly crystalline to an amorphous structure. The material was deposited onto borosilicate glass for electrical and Raman measurements, and on Si-wafers for infrared measurements. For ESR measurements, the material was deposited on Mo foil and glass substrates. Samples peeled off in flakes when the Mo foil was bent, and were sealed in a He atmosphere in quartz tubes. The influence of different environments during storage or annealing was studied by removing the samples from the He filled tubes and sealing them in an Ar or O_2 atmosphere, or treating them in water. The ESR was measured at X-band, at room temperature or at 40 K. Infrared spectroscopy was performed on co-deposited samples on Si-wafers. The electrical conductivity was measured with coplanar contacts in vacuum, soon after deposition. The current-voltage characteristic was measured to assure Ohmic contact behaviour. Samples were studied between 200K and 450K, in vacuum. They were stored alternatively in vacuum or under atmosphere for certain periods of time, and then re-measured.

3. Results

3.1. Infrared Spectroscopy

The effect of the pronounced porosity is easily observed in the IR spectra. In Fig. 2, the IR spectra of two $\mu\text{c-Si:H}$ samples are shown. The Raman intensity ratios I_c^{RS} , as semi-quantitative measures of the crystalline volume fraction [11] are indicated in the figure. The type I sample shows very strong Si-O modes around 1100cm^{-1} , and a high 2100cm^{-1} absorption mode indicative of Si-H surface states. An additional absorption band at $2240\text{-}2250 \text{cm}^{-1}$ is found, which is related to $\text{O}_{2...3}\text{-Si-H}$ [12]. The Si-O mode shows a clear time dependence and is not observed when the sample is measured directly after deposition or after storage in inert gas or N_2 . The type II sample with compact material shows little or no Si-O mode, and is stable with time. Also, the 2000cm^{-1} mode dominates over the 2100cm^{-1} mode. Note that the type II (compact) sample has a higher I_c^{RS} , which

underlines the problematic distinction of the material into type I and II categories. Similar observations, i.e. indications for a strong oxidation effect in a porous material, have been made with $\mu\text{-Si:H}$ prepared by PECVD [5, 6, 9, 10]

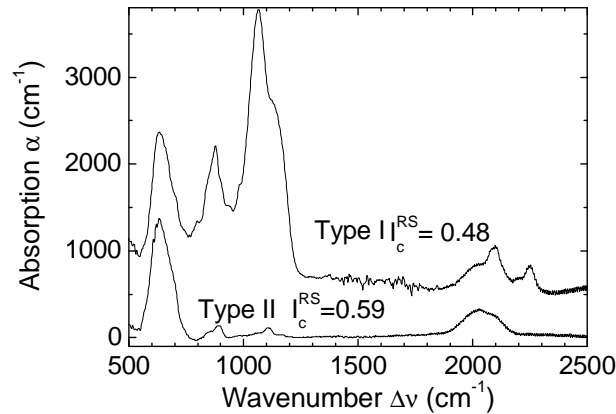


Fig. 2. Infrared absorption spectra of two $\mu\text{-Si:H}$ type I and type II films prepared by HWCVD. The spectra are shifted with respect to each other, for clarity.

3.2. Electrical conductivity

Type I and type II $\mu\text{-Si:H}$ samples show distinctly different influences of storage in air and annealing on the electronic dark conductivity σ_D . In Fig. 3, the dark conductivity σ_D is shown as a function of $1000/T$ for the two samples in Fig. 1. After the storage in air of sample type I, the conductivity decreases by up to 3 orders of magnitude. After annealed in vacuum at 180°C , the initial σ_D is restored. σ_D remains at this value when the sample is kept in vacuum. The conductivity decreases again when the sample is put back into air. This cycle can be repeated many times, without any sign of fatigue (compare with ref. [4]).

Type II samples show a different behaviour. When put in air, the conductivity increases. Again this change in σ_D can be restored when the sample is annealed in vacuum at 180°C . The conductivity remains at this level when kept in vacuum, and increases when the sample is exposed to air. For type II the cycles can again be repeated many times.

Similar observations have been made for material prepared by PECVD [13-16].

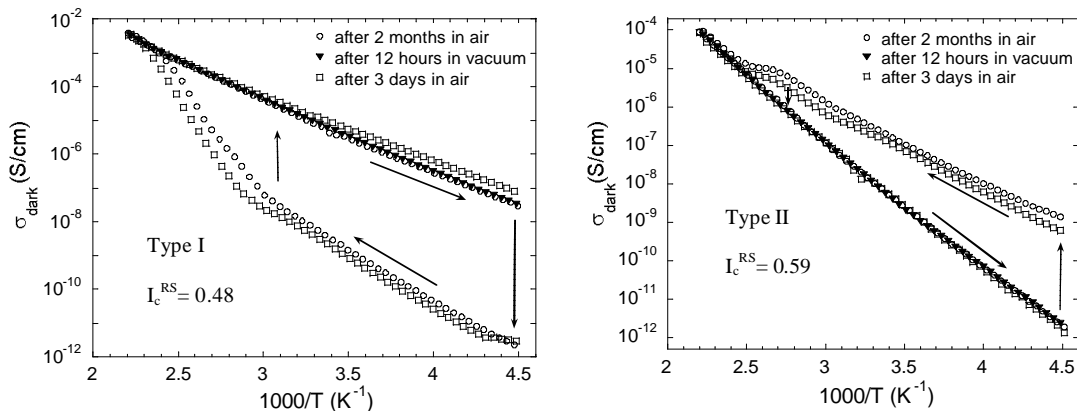


Fig. 3. Dark conductivity of (left) type I and (right) type II samples from Fig 1, during various annealing and storage cycles.

3.2. Electron Spin Resonance

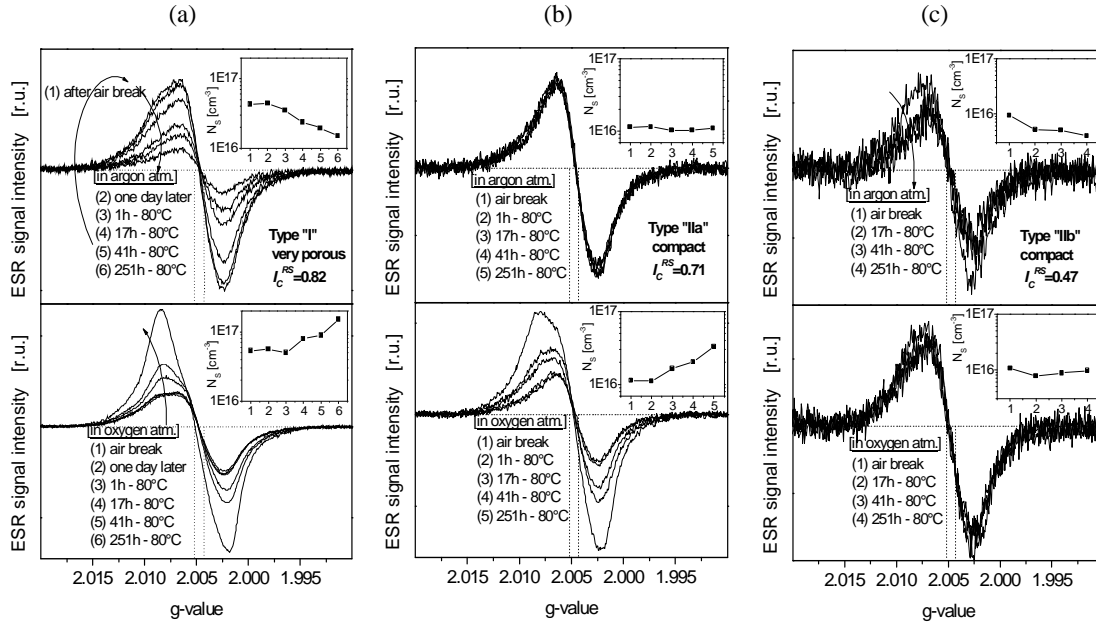


Fig. 4. ESR signals and spin densities of (a) type I, highly crystalline and porous, (b) type IIa, highly crystalline and compact, and (c) type IIb, from the transition between amorphous and crystalline growth and compact material. The samples were divided into two parts of approximately equal mass, and were annealed in Ar or O₂ atmospheres respectively, after exposure to air.

The powder material for the ESR measurements was deposited on Mo foil. The material peeled off easily when the foil was bent after deposition, and the powder could be collected into quartz tubes and sealed in an inert gas atmosphere within a short time. Thus, prolonged exposure of the powder to air, water or solvents, as in the case of the alternative deposition of powder material on Al foil [10, 16-18], could be avoided. To investigate the influence of gas adsorption or oxidation on $\mu\text{c-Si:H}$ material with different structural properties in a controlled manner, the powder could also be sealed in the respective gas atmospheres like oxygen.

In Fig. 4 a-c, the influence of storage of PECVD $\mu\text{c-Si:H}$ powder of type I and type II in air, Ar or O₂ and subsequent annealing on the ESR signal is shown. The original untreated material shows the well known ESR signal of undoped $\mu\text{c-Si:H}$, with contributions at $g = 2.0043$ and 2.0052 with line widths of about 6-8 G [16-18]. The microscopic origins of these two resonances are still not clear. However, as we will show, the experiments described in the present report may help in the identification of the corresponding states, and in their location in the material.

For type I material, the initial spin density obtained after sealing the sample in He atmosphere increased considerably after the quartz tubes were broken and the material was exposed to air under ambient conditions for a few hours (Fig. 4a). When the material was refilled into an Ar atmosphere and annealed at 80°C, the initial lower spin density values could be restored. This cycle could be repeated several times. Spectral analysis showed that the changes occurred mainly for the line contribution at $g = 2.0052$ [16]. In principle, there are two explanations for this observation: (i) the creation and annealing of additional defects at $g = 2.0052$, and (ii) a change in the occupation of the corresponding states, via a Fermi level shift. We shall discuss this below.

Type II material shows very little or no change upon exposure to air and annealing in Ar, in highly crystalline but compact material, which we will call Type "IIa" (Fig. 4b). In compact material grown close to the transition between amorphous and crystalline growth conditions (Type "IIb") we observed little decrease in N_S with annealing in Ar (Fig. 4c).

On the other hand, when the material was annealed in oxygen at 80°C, there was a non-reversible change of the spin density for type I and type IIa material (Fig. 4a&b). Type IIb material

showed no effect upon annealing in oxygen (Fig. 4c). The spin density change happened at a higher g -value, and a different spectral shape could be observed. The increase in N_S upon annealing in O_2 or air in porous type I material could be restored by an HF dip. This is shown in Fig. 5. In this case, for ease of sample handling, a sample on glass was used. With the reduced sample volume, the signal to noise ratio was considerably lower. Still, one could easily observe the increase in N_S after annealing in air and the recovery after etching in HF. Because of the low signal intensity, the signal was superimposed by signal traces from the borosilicate glass substrate, at around $g = 2.001$.

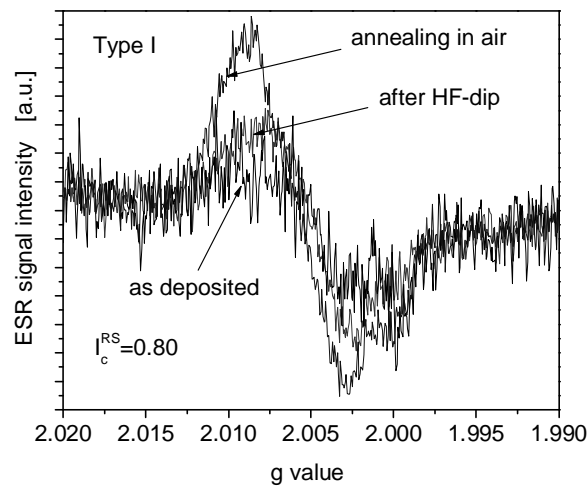


Fig. 5. ESR signal of a porous $\mu\text{c-Si:H}$ type I sample deposited on a glass substrate, and after annealing in air and after HF etching.

4. Discussion

The instability and metastability phenomena in $\mu\text{c-Si:H}$ are numerous, and should be a matter of great concern for the understanding of the material properties as well as for possible technological applications of these materials.

Apparently, the porous structure of type I material leads to in-diffusion of atmospheric gases, which results in changes in the electrical conductivity and the spin density. The results show many similarities with those reported earlier [4]. For type II material, we are not aware of any previous detailed reports in the literature.

In the meantime, adsorption or oxidation related effects have been also studied in $\mu\text{c-Si:H}$ solar cells prepared by HWCVD and PECVD [19, 20]. In each group, there were cells prepared under conditions close to the transition to amorphous growth, resulting in compact material, and cells containing high crystalline volume fraction material. The cells were first annealed in vacuum or in dry air at 160°C . They were then treated in de-ionized water at 80°C for different lengths of time, stored under ambient conditions and annealed again. A strong degradation of the J-V parameters of cells with highly crystalline i-layers was observed after treatment in de-ionized water. The cells with a compact i-layer material, on the other hand, showed very little changes of their J-V parameters [19-20].

We will briefly discuss how far the various observed meta-stability and instability effects in $\mu\text{c-Si:H}$ of various structural compositions can be related to each other and/or have the same origin. The main effects to consider are adsorption and oxidation on surfaces.

Let us first compare the magnitude of the involved states which lead to the observations in IR, conductivity and ESR studies. To be detectable in such a quantity as the Si-O absorption mode in the IR spectra of Fig. 2, the number of Si-O bonds has to be of the order of a few tenths of a percent of the total number of bonds, which means a few times 10^{19}cm^{-3} . This has to be compared with the 10^{16} - 10^{17}cm^{-3} spin states which appear as additional signal contributions in the ESR experiments.

With a mobility gap defect density of a few times $10^{16} \text{cm}^{-3} \text{eV}^{-1}$, the creation or recharging of a similar numbers of states in the gap has a considerable influence on the Fermi level position, which results in the observed changes in the conductivity. Therefore the changes which are observed in the ESR or conductivity are typically related to many fewer states than those involved in the changes in Si-O bonding which are detected in the IR spectra.

4.1. Oxidation

The presence of the Si-O absorption mode at around 1100cm^{-1} indicates an oxidation process of $\mu\text{c-Si:H}$ material of type I. The magnitude of the Si-O mode is linked to the magnitude of the 2100cm^{-1} absorption, which is indicative of Si-H surface states in the crystalline material. This oxidation process is thermally activated. It already starts at room temperature, but is considerably faster at 80°C . The resulting Si-O bonds are stable, i.e. the process is non-reversible up to annealing temperatures of 200°C . Vepřek *et al.* report the removal of the oxygen only above 1050°C [4]. The non-reversible occurrence of additional spins upon annealing in oxygen can be related to this oxidation process. Si-O/Si interface dangling bond defects (P_b centres) are the most likely candidates for this defect. If such an interpretation is correct, apparently only a fraction (10^{16} to 10^{17}cm^{-3} of 10^{20}cm^{-3}) of the Si-O states observed in the IR give rise to spin related states. The fact that the increase of N_S after annealing in O_2 or air can be restored with an HF dip supports the conclusion that this is a surface process. Note that by “surface” we refer to the surface of cracks within the film structure, and not merely to the macroscopic film surface.

Compact type II material, on the other hand, is not at all or much less affected by this oxidation process, at least the effects are not visible in the IR. On the other hand, ESR does see an increase of a possibly Si-O related state upon annealing in oxygen, of the order of $3 \times 10^{16} \text{cm}^{-3}$ for type IIa material (Fig 4b). Finally, compact material with a significant amorphous phase (type IIb) shows no effect of oxidation in IR and ESR measurements.

Studies of the influence of irreversible oxidation on the conductivity in our material are under way [15]. It will have to be seen whether the magnitude of the reversible changes is influenced by the amount of irreversible oxidation of the material [4].

4.2. Adsorption

Compared with the non-reversible oxidation effects, the effects of adsorption on the conductivity and ESR signals are reversible by moderate temperature annealing in inert gas, or by long time storage in inert gas or in vacuum. These effects can still be observed after many cycles, with no sign of fatigue or accumulation of any irreversible effect. They can be related to the adsorption of water or O_2 [4]. Unlike the irreversible oxidation of type I material, the reversible adsorption can not be detected in the IR spectra. The intensity is too low, or the involved states are infrared vibrationally inactive [4].

The reversible change in N_S is only observed in type I material, although all these ESR experiments apart from the HF dip were performed on powder material with a presumably large macroscopic surface area. Apparently, the large surface area of the powder is not similar to the internal surface of the material with strong porosity of the type I structure. On the other hand, the structure and reactivity of the internal surfaces of the porous material could be different from the macroscopic surfaces of the material.

As to the origin of the reversible changes in the ESR signal, one can only speculate. The thermal energies during storage and annealing of the samples are too low for breaking up and annealing of e.g. Si-db. If adsorption leads to strong band bending, this could result in bond breaking via the weak-bond (WB) - dangling-bond conversion, similar to the field effect and doping induced defect creation in a-Si:H [21]. However, it is difficult to associate the WB-db conversion to the up- and down-changes of σ_D and N_S . Band bending can also result in a change of the occupation of states which make the transition from diamagnetic to paramagnetic. Any explanation should consider the corresponding changes in the conductivity. If conductivity changes are induced by shifts of the Fermi level, this will also change the occupation of states and in general will change the ESR signal.

For the conductivity changes, one can assume adsorption of oxygen or water [4]. The two samples for which conductivity was measured here were both undoped. Such material generally shows n-type conduction, as determined by the Hall effect. The adsorption of an electron acceptor molecule will create a depletion layer at the surface, which will result in a lower overall conductivity. This is equivalent to a movement of the Fermi level away from the conduction band. States in the upper half of the gap get depopulated. When these states change their occupation from (let us say) D^- (two electrons, no ESR) to D^0 (one electron, ESR), one would observe an increase in the ESR signal. The details are difficult to predict, as they will depend on the relationships between the effective correlation energy of the defects, plus the energy positions and the distributions in energy. What supports the picture of a change in occupation is:

1) The changes occur at $g = 2.0052$, a line contribution which is found together with the superimposed signal at $g = 2.0043$ in all our $\mu\text{c-Si:H}$ material [16-18]. We consider it as originating from an intrinsic Si-db defect in the material.

2) Various findings, like the parallel existence of the db ($g = 2.0043/52$) and CE ($g = 1.996$) states and the broad distribution in energy of the $g = 2.0052$ state upon a shift of the Fermi level by doping [16-18, 22], suggest that the $g = 2.0052$ states are located in the upper half of the mobility gap, possibly only in parts of the material.

An alternative explanation for the increase of the $g = 2.0052$ resonance would relate the resonance to states of the adsorbed species [4]. Further studies will be needed to conclusively decide between these explanations.

The changes in σ_D in type II material remind one of similar effects known from high quality undoped a-Si:H, which shows a higher σ_D if exposed to the ambient atmosphere. This corresponds to an accumulation layer induced by adsorption. Different grades of passivation of the surface states between type I and type II material could be the reason for the two opposite trends in σ_D . We note that for compact type IIb material, there is only a small decrease of N_S upon exposure to air (Fig. 4c). Whether this can be related to the increase in σ_D will have to be investigated.

The rather strong effect on σ_D in both directions should be considered carefully in routine measurements. A standard annealing procedure in vacuum seems compulsory for a reliable and reproducible measurement. Similarly, one should consider these effects for the evaluation of the spin density. Also, long term stability could be a matter of concern for the transport behaviour of the $\mu\text{c-Si:H}$ material [15]. Finally the observation of related instability effects in solar cells [19, 20] should be considered for device applications.

5. Conclusions

In $\mu\text{c-Si:H}$ prepared by HW- and PE-CVD we observe various reversible and irreversible changes which effect the structure and electronic properties of the material and the corresponding solar cells. The phenomena depend strongly on the structural composition of the material. Adsorption and oxidation, which can be observed in IR, σ_D and ESR measurements, show many similarities to the earlier investigations made on material which was grown by the chemical transport technique [4]. There are, however, some additional effects which have not been described before. Investigation of these phenomena should be given serious attention in the future.

Acknowledgements

We are thankful to W. Beyer, M. Hülbeck, A. Lambertz, S. Michel and J. Wolff for valuable contributions. For parts of this work, financial support by the International Bureau of the BMBF, Germany under project number 42.4.I3B.2.A and the Scientific and Technical Research Council of Turkey (TÜBİTAK), under project number, TBAG-U/14 is kindly acknowledged.

References

- [1] O. Vetterl, F. Finger, R. Carius, P. Hapke, L. Houben, O. Kluth, A. Lambertz, A. Mück, B. Rech, H. Wagner, *Solar Energy Materials and Solar Cells* **62**, 97 (2000).
- [2] S. Klein, J. Wolff, F. Finger, R. Carius, H. Wagner, M. Stutzmann, *Jpn. J. Appl. Phys. Part II: Letters* **41**, L10 (2002).
- [3] Y. Mai, S. Klein, X. Geng, F. Finger, *Appl. Phys. Lett.* **85**, 2839 (2004).
- [4] S. Veprék, Z. Iqbal, R. O. Kühne, P. Capezzuto, F. -A. Sarott, J. K. Gimzewski, *J. Phys. C* **16**, 6241 (1983).
- [5] H. Curtins, S. Veprék, *Solid State Comm.* **57**, 215 (1986).
- [6] P. Hapke, unpublished, (1997).
- [7] R. Brüggemann, A. Hierzenberger, H. N. Wanka, M. B. Schubert, *Mat. Res. Soc. Symp. Proc.* **507**, 921 (1998).
- [8] P. Kanschat, K. Lips, R. Brüggemann, A. Hierzenberger, I. Sieber, W. Fuhs, *Mat. Res. Soc. Symp. Proc.* **507**, 793 (1998).
- [9] A. Mück, U. Zastrow, O. Vetterl, B. Rech, *Secondary Ion Mass Spectrometry SIMS XII*, ed. by A. Benninghoven, P. Bertrand, H.-N Migeon and H.W. Werner, Elsevier Science B.V., Amsterdam, 689 (2000).
- [10] T. Dylla, F. Finger, R. Carius, *Mat. Res. Soc. Symp. Proc.* **762**, A2.5 (2003).
- [11] L. Houben, M. Luysberg, P. Hapke, R. Carius, F. Finger, H. Wagner, *Phil. Mag. A* **77**, 1447 (1998).
- [12] N. Kniffler, B. Schröder, J. Geiger, *J. Non-Cryst. Solids* **58**, 153 (1983).
- [13] V. Smirnov, S. Reynolds, F. Finger, C. Main, R. Carius, *Mat. Res. Soc. Symp. Proc.* **808**, A9.11 (2004).
- [14] V. Smirnov, S. Reynolds, C. Main, F. Finger, R. Carius, *J. Non-Cryst. Solids* **338-340** 412 (2004).
- [15] S. Reynolds, V. Smirnov, F. Finger, C. Main, R. Carius, this volume.
- [16] T. Dylla, Thesis, Forschungszentrum Jülich and Freie Universität Berlin (2004).
- [17] F. Finger, J. Müller, C. Malten, H. Wagner, *Phil. Mag. B* **77**, 805 (1998).
- [18] J. Müller, F. Finger, R. Carius, H. Wagner, *Phys. Rev. B* **60**, 11666 (1999).
- [19] M. Sendova-Vassileva, S. Klein, A. Lambertz, F. Finger, *Proc. 19th European Photovoltaic Solar Energy Conference and Exhibition, Paris* (2004).
- [20] M. Sendova-Vassileva, F. Finger, S. Klein, A. Lambertz, this volume
- [21] M. Stutzmann, *Phil. Mag. B* **60**, 531 (1989).
- [22] T. Dylla, R. Carius, F. Finger, *Mater. Res. Soc. Symp. Proc.* **715**, A20.9 (2002).